Femtosecond pulse synthesis by efficient second-harmonic generation in engineered quasi phase matching gratings

Usman K. Sapaev and Gaetano Assanto

Nonlinear Optics and OptoElectronics Lab, INFN & CNISM, University Roma Tre
Via della Vasca Navale 84, 00146, Rome- Italy
http://optow.ele.uniroma3.it

Abstract: We numerically design quasi-phase matched crystals with domains of arbitrary sizes for second harmonic generation by femtosecond pulses, taking into account both group velocity mismatch and dispersion. An efficient simulated-annealing algorithm is developed to design quasi-phase matching gratings which can yield the desired amplitude and phase of second-harmonic pulses in the presence of pump depletion. The method is illustrated with reference to single, double-hump and chirped fs Gaussian pulses in a lithium niobate crystal.

OCIS codes: (190.2620) Nonlinear optics (frequency conversion); (190.4400) Nonlinear optics (materials)

References and links

1. J. A. Armstrong, N. Bloembergen, J. Ducuing and P. S. Pershan, "Interactions between Light Waves in a Nonlinear Dielectric," Phys. Rev. **127**, 1918-1939 (1962).
2. M. A. Arbore, O. Marco and M. M. Fejer, "Pulse compression during second-harmonic generation in aperiodic quasi-phase-matching gratings," Opt. Lett. **22**, 865-867 (1997).
3. M. A. Arbore, A. Galvanauskas, D. Harter, M. H. Chou and M. M. Fejer, "Engineerable compression of ultra-short pulses by use of second-harmonic generation in chirped-period-poled lithium niobate," Opt. Lett. **22**, 1341-1343 (1997).
4. D. Artigas, D. T. Reid, M. M. Fejer and L. Torner, "Pulse compression and gain enhancement in a degenerate optical parametric amplifier based on aperiodically poled crystals," Opt. Lett. **27**, 442-444 (2002)
5. D. Artigas and D. T. Reid, "Efficient femtosecond optical parametric oscillators based on aperiodically poled nonlinear crystals," Opt. Lett. **27**, 851-853 (2002).
6. M. M. Fejer, G. A. Magel, D. H. Jundt and R. L. Byer, "Quasi-phase-matched second harmonic generation - Tuning and tolerances," IEEE J. Quantum Electron. **28**, 2631-2653 (1992).
7. P. Loza-Alvarez, D. T. Reid, P. Faller, M. Ebrahimzadeh and W. Sibbett, "Simultaneous second-harmonic generation and femtosecond-pulse compression in aperiodically poled $KTiOPO_4$ with a $RbTiOAsO_4$ -based optical parametric oscillator," J. Opt. Soc. Am. B **16**, 1553-1560 (1999).
8. P. Loza-Alvarez, D. T. Reid, P. Faller, M. Ebrahimzadeh, W. Sibbett, H. Karlsson and F. Laurell, "Simultaneous femtosecond-pulse compression and second-harmonic generation in aperiodically poled $KTiOPO_4$," Opt. Lett. **24**, 1071-1073 (1999).
9. T. Beddard, M. Ebrahimzadeh, D. T. Reid and W. Sibbett, "Five-optical-cycle pulse generation in the mid infrared from an optical parametric oscillator based on aperiodically poled lithium niobate," Opt. Lett. **25**, 1052- 1054 (2000).
10. G. Imeshev, M. A. Arbore, M. M. Fejer, A. Galvanauskas, M. Fermann and D. Harter, "Ultrashort-pulse second-harmonic generation with longitudinally nonuniform quasi-phase-matching gratings: pulse compression and shaping," J. Opt. Soc. Am. B **17**, 304-318 (2000).
11. G. Imeshev, M. A. Arbore, S. Kasriel and M. M. Fejer, "Pulse shaping and compression by second-harmonic generation with quasi-phase-matching gratings in the presence of arbitrary dispersion," J. Opt. Soc. Am. B **17**, 1420-1437 (2000).
12. R. Buffa, "Transient second-harmonic generation with spatially non-uniform nonlinear coefficients," Opt. Lett. **27**, 1058-1060 (2002).
13. R. Buffa and S. Cavalieri, "Optimal control of type I second-harmonic generation with ultrashort laser pulses," J. Opt. Soc. Am. B **17**, 1901-1905 (2000).

#82198 - $15.00 USD Received 17 Apr 2007; revised 26 May 2007; accepted 27 May 2007; published 1 Jun 2007

14. M. Conforti, F. Baronio and C. De Angelis, "From femtosecond infrared to picosecond visible pulses: temporal shaping with high efficiency conversion," Opt. Lett. (to appear).
15. S. Helmfrid and G. Arvidsson, "Influence of randomly varying domain lengths and non-uniform effective index on second-harmonic generation in quasi-phase-matching waveguides," J. Opt. Soc. Am. B **8**, 797-805 (1991).
16. D. T. Reid, "Engineered quasi-phase-matching for second-harmonic generation," J. Opt. A: Pure Appl. Opt. **5,** S97-S102 (2003).
17. U. Sapaev and D. T. Reid, "General second-harmonic pulse shaping in grating-engineered quasi-phase-matched nonlinear crystals," Opt. Express **13,** 3264-3276 (2005) http://www.opticsinfobase.org/abstract.cfm?URI=oe-13-9-3264
18. U. Sapaev, "Optimum shaping of a spectral response of second harmonic generation process in the aperiodic quasi-phase matched nonlinear crystal," Opt. Spectrosc. **102**, 1023-1027 (2007).
19. E. A. Morozov, A. A. Kaminski, A. S. Chirkin and D. B. Yusupov, "Second optical harmonic generation in nonlinear crystals with a disordered domain structure," JETP Lett. **73,** 647–650 (2001).
20. W. H. Press, S. A Teukolsky, W. T. Vetterling and B. P. Flannery "*Numerical Recipes*", 2nd end (Cambridge University Press).
21. R. A. Fisher and W. K. Bischel, "Numerical studies of the interplay between self-phase modulation and dispersion for intense plane-wave laser pulses," J. Appl. Phys. **46**, 4921-4934 (1975).
22. E Sidick, A Knoesen and A Dienes, "Ultrashort-pulse second-harmonic generation. I: Transform-limited fundamental pulses," J. Opt. Soc. Am. B **12**, 1704-1712 (1995).
23. N. C. Kothari and X. Carlotti "Transient second-harmonic generation: influence of effective group-velocity dispersion," J. Opt. Soc. Am. B **5**, 756-764 (1988).
24. Y. Zang and B-Y. Gu, "Optimal design of aperiodically poled lithium niobate crystals for multiple wavelengths parametric amplification," Opt. Commun. **192**, 417-425 (2001).
25. V. G. Dmitriev G. G. Gurzadyan, and D. N. Nikogosyan, *Handbook of Nonlinear Optical Crystals*, Springer, Berlin (1999).

1. Introduction

Various nonlinear optical media are used for converting a laser frequency to the required wavelength, where direct laser emission is impossible or available at low energies. Quasi-phase-matched (QPM) crystals with a second order susceptibility are of great interest in practical applications, because they do not require the phase matching necessary in uniform nonlinear crystals [1]. In QPM crystals phase matching (or phase synchronism) of the interacting waves is obtained by periodically changing the sign of the second-order susceptibility, effectively widening the spectral range of frequency converters. It was also recognized that QPM gratings can provide dramatic pulse compression [2-3] and improved conversion efficiencies [4-5].

In the presence of a non-uniform periodicity, QPM gratings exhibit a longitudinally variable spectral response and entail the realization of advanced parametric processes [6], from highly efficient second harmonic generation (SHG) and parametric amplification in the case of a linear QPM chirp [4-5,7-9], to compression of second harmonic (SH) pulses when employing chirped fundamental-frequency (FF) pulses, [2-3, 10-11].

One of the challenges in engineering QPM gratings is the generation of SH pulses (or other parametrically generated frequencies) with arbitrarily chosen amplitude and phase profiles under the regime of pump depletion, i.e. when large energy conversion is sought. A few methods have been developed to this extent. Among them the optimal control technique, based on Lagrange multipliers and real amplitudes [12-13], was applied to tailor ultra-short SH pulses by spatially varying the size of the nonlinearity. More recently, a similar approach was employed to design QPM gratings for picosecond SHG from femtosecond input FF pulses [14]. The role of arbitrary size domains in aperiodic QPM gratings for SHG has been addressed with various approaches, investigating the effect of fabrication errors [15], the generation of a spectral distribution in the un-depleted pump approximation [16-17] or in the depleted pump regime without GVD or GVM [18]. SHG in aperiodic nonlinear crystals with domains of arbitrary sizes was also developed within the stochastic theory of waves in Ref. [19].

#82198 - $15.00 USD Received 17 Apr 2007; revised 26 May 2007; accepted 27 May 2007; published 1 Jun 2007

In this paper we discuss arbitrary fs pulse shaping based on SHG in engineered QPM in the regime of strongly depleted FF pump, taking into account both group velocity mismatch (GVM) and dispersion (GVD). To this extent, at variance with previous work on the topic, we employ a simulated annealing algorithm (SAA), using simple fast Fourier transform and fourth-order Runge–Kutta algorithms.

The outline is as follows: Section 2 describes the theoretical model; Section 3 the conditions (material, wavelength) in which the design of femtosecond SH pulses is illustrated. Section 4 presents numerical results and discussion.

2. Coupled-wave equations for SHG in arbitrary QPM gratings

The slowly varying envelope equations describing pulse evolution under collinear SHG in QPM are:

$$\begin{aligned}
&\frac{\partial A_1}{\partial z}+\frac{1}{V_1}\frac{\partial A_1}{\partial t}-i\frac{\alpha_1}{2}\frac{\partial^2 A_1}{\partial t^2}=-i\gamma_1\delta(z)(A_1)^* A_2\exp(-i\Delta kz)\\
&\frac{\partial A_2}{\partial z}+\frac{1}{V_2}\frac{\partial A_2}{\partial t}-i\frac{\alpha_2}{2}\frac{\partial^2 A_2}{\partial t^2}=-i\gamma_2\delta(z)(A_1)^2\exp(i\Delta kz)
\end{aligned} \tag{1}$$

with boundary conditions

$$\begin{aligned}
&A_1(z,t)\big|_{z=0}=A_o\exp(-2\ln 2(t/\tau)^2+i\varphi_1)\\
&A_2(z,t)\big|_{z=0}=0
\end{aligned} \tag{1a}$$

being A_1 and A_2 the complex amplitudes of FF and SH pulses, respectively; A_o the peak amplitude of the FF excitation; V_1 and α_1 (V_2 and α_2) the group velocity and the dispersive (GVD) spreading at FF (SH), respectively; τ input pulse duration (FWHM in intensity); γ_1 and γ_2 nonlinear coupling coefficients, with $\gamma\approx\gamma_1\approx\gamma_2\approx\frac{2\pi}{n(\omega_o)\lambda}d^{eff}\approx\frac{2\pi}{n(2\omega_o)\lambda}d^{eff}$; $n(\omega_o)$ and $n(2\omega_o)$ the refractive indices of FF and SH waves, respectively; d^{eff} the effective nonlinearity $d^{eff}=\chi^{(2)}/2$; $\Delta k=2k_1(\omega_o)-k_2(2\omega_o)$ the phase-mismatch; φ_1 an initial FF phase and $\delta(z)$ the unitary sign-changing function defining the arbitrarily sized domains of the QPM grating (see Fig. 1).

It is convenient to recast Eq. (1) in a dimensionless form as:

$$\begin{aligned}
&\frac{\partial a_1}{\partial\xi}-i\beta_1\frac{\partial^2 a_1}{\partial\mu^2}=-i\delta(\xi)(a_1)^* a_2\exp(-i\Delta S\xi)\\
&\frac{\partial a_2}{\partial\xi}+\rho\frac{\partial a_2}{\partial\mu}-i\beta_2\frac{\partial^2 a_2}{\partial\mu^2}=-i\delta(\xi)(a_1)^2\exp(i\Delta S\xi)
\end{aligned} \tag{2}$$

with boundary conditions

$$\begin{aligned}
&a_1(\xi,\mu)\big|_{\xi=0}=exp(-2\ln 2\mu^2+i\varphi_1)\\
&a_2(\xi,\mu)\big|_{\xi=0}=0
\end{aligned} \tag{2a}$$

where $a_1=A_1/A_o$ and $a_2=A_2/A_o$, $\mu=t/\tau$, $\nu=1/V_2-1/V_1$, $L_{NL}=1/(A_o\gamma)$, $\xi=z/L_{NL}$, $\rho=\nu L_{NL}/\tau$, $\beta_i=\alpha_i L_{NL}/\tau^2/2$ i=[1,2], $\Delta S=\Delta kL_{NL}$, $I_o=n(\omega_o)|A_o|^2/2Z_o$ and Z_o is the vacuum impedance.

#82198 - $15.00 USD Received 17 Apr 2007; revised 26 May 2007; accepted 27 May 2007; published 1 Jun 2007

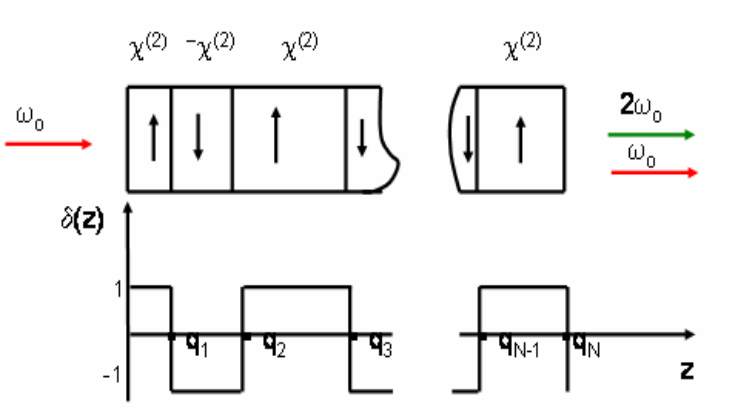

Fig. 1. Scheme of the arbitrary QPM grating, with δ(z) the dimensionless sign-changing aperiodic function of amplitude |δ(z)| = 1. The grating is comprised of N inverted domains with individual lengths q_m ($1 \le m \le N$).

The set (2) could be numerically integrated by various methods. The fast Fourier transform for the linear portion and the fourth-order Runge–Kutta (RK) method for the nonlinear one ensure high accuracy and reduced iteration times [21-23], However, because of the aperiodic nature of δ(ξ), we resort to RK with variable integration steps $d\xi(m)$ (m is the domain number**)** inside each domain (see Fig. 2). GVM and GVD are accounted by the fast Fourier transform as in Ref. [22].

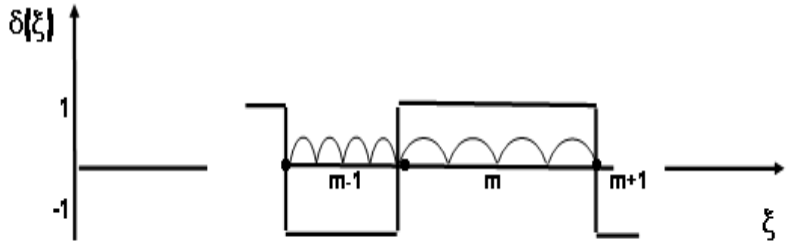

Fig. 2. Integration scheme. Here the number of steps in each domain is j=4.

In order to ascertain the capability of the numerical approach, we initially neglected both GVM and GVD. As an example, Fig. 3 graphs the SHG energy conversion (left) and the variation in domain sizes (right) versus grating length for various QPM gratings. The results are displayed for ρ=0, β_i=0, l_o=0.1, ΔS=π/l_o, N=15, j=5, L_{NL}=1, with l_o being the coherence length for SHG, N the total number of domains, j is the number of steps inside each domain. In the uniform case, SHG conversion (black line) monotonically increases with crystal length, as expected. Conversely, the introduction of grating chirp (red and blue lines) or randomness (green and magenta lines) completely changes the character of energy transfer between FF and SH.

#82198 - $15.00 USD Received 17 Apr 2007; revised 26 May 2007; accepted 27 May 2007; published 1 Jun 2007

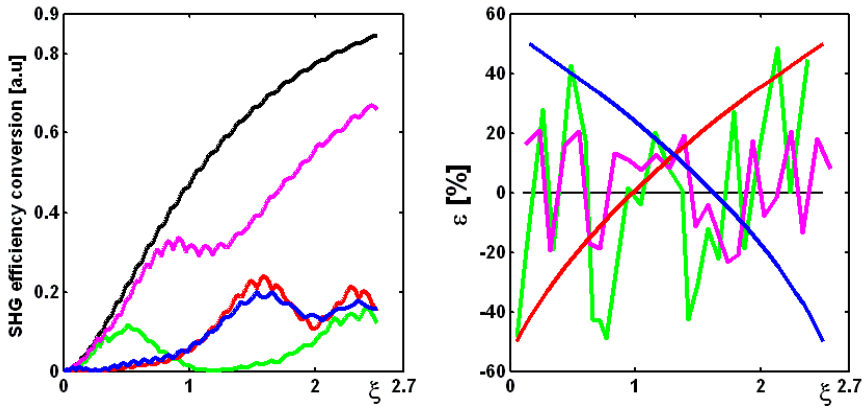

Fig. 3. (Left) Normalized SHG conversion and (Right) domain size variation versus normalized crystal length (units of L_{NL}), for various QPM conditions: black lines, uniform grating; blue lines, positively chirped; red lines, negatively chirped; green and magenta lines, randomly varied. Here $\varepsilon=100*(q_m-l_o)/l_o$.

3. Designing femtosecond SH pulses of desired amplitude and phase profiles

Our goal is to synthesize by SAA any prescribed SH target pulses by defining the length of each susceptibility domain and the total number of domains in the QPM grating [16-18, 20, 22, 24]. We summarize below the main lines of the SAA algorithm we used [17, 20] starting with a uniform QPM grating defined by N=10 and $\Lambda=2l_0$:

1. Given a target SH profile, calculate its polarization-gated frequency-resolved optical gating (PG-FROG) trace;
2. Calculate the SH output pulse by integrating Eqs. 2 and the corresponding PG-FROG trace;
3. Calculate the root-mean-square (RMS) error between calculated and target profiles from their PG-FROG traces;
4. Apply a random perturbation of domain sizes up to 1% and vary the total number of domains, adding (subtracting) one if the final conversion efficiency is lower (higher) than the target value; re-calculate the SH output pulse and its PG-FROG trace;
5. Re-calculate the RMS error between calculated and target SH profiles from their PG-FROG traces and, depending on its magnitude as compared to the previous iteration, proceed by perturbing the last QPM distribution or the previous one, according to SAA rules [17, 20];
6. Repeat steps 4-5 until the RMS error becomes as small as desired.

It is worth stressing that, although one could calculate the RMS error on either temporal or spectral profiles of calculated and desired SH pulses, the PG-FROG traces allows us to simultaneously compute the RMS error in time and spectrum, making the SAA method very efficient.

In order to demonstrate the applicability of approach, we used 100 fs incident Gaussian pulses (FWHM in intensity) launched at a wavelength of 1550 nm and with peak intensity 5.0 GW/cm^2 in a z-cut $LiNbO_3$ crystal ($d^{eff}=d_{33}$=30pm/V [25]). The QPM period is $\Lambda_o=2l_o$=18.26 μm, with GVM $\nu\approx$0.3 ps/mm and GVD $\alpha_1\approx0.1\cdot10^{-3}$ ps^2/mm, $\alpha_2\approx0.4\cdot10^{-3}$ ps^2/mm at FF and SH, respectively.

#82198 - $15.00 USD Received 17 Apr 2007; revised 26 May 2007; accepted 27 May 2007; published 1 Jun 2007

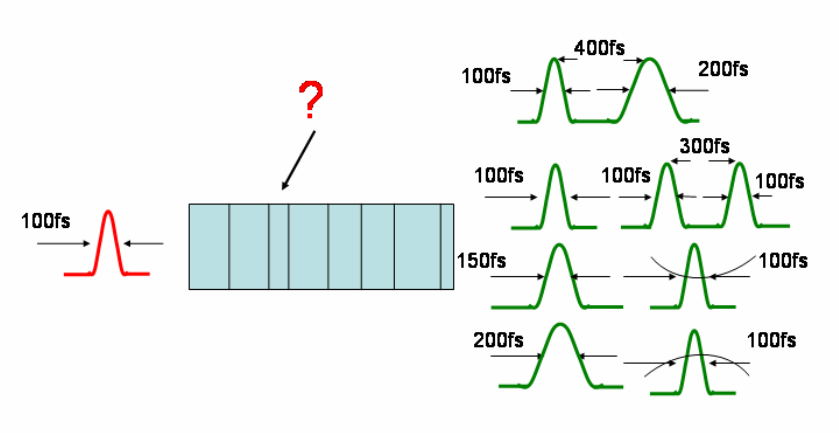

Fig. 4. Illustration of the synthesis task. A fundamental frequency Gaussian shaped pulse (red profile) excites with duration τ=100 fs and peak intensity I_0=5 GW/cm^2 the QPM structure to be determined (blue box) in order to generate the desired SH target pulses (green profiles on the right).

Although, the FF pulse could be preventively shaped or chirped to facilitate the SAA task, we aim hereby at demonstrating how powerful the procedure is in the synthesis of the desired targets at SH for one and the same "standard" FF input. We considered seven SH profiles differing in amplitude and phase, as illustrated in Fig. 4: (i) a 100 fs Gaussian pulse; (ii) a 150 fs Gaussian pulse; (iii) a 200 fs Gaussian pulse; (iv) a double-humped profile with 100 fs pulses with peaks separated by ~300 fs; (v) a double pulse with 100 and 200 fs FWHM with peaks separated by ~400 fs; (vi) a positively chirped 100 fs Gaussian pulse (ϕ''~150 fs^2); (vii) a negatively chirped 100 fs Gaussian pulse (ϕ''~-150 fs^2). For all targets we aimed at SHG conversion efficiencies close to 50%, although higher values could be obtained. The SAA algorithm typically run for times ranging from 0.5 to 4 hours on a standard PC, depending on the SH target.

4. Results and discussion

Figure 5(a) shows the results obtained for the case (i) above, i. e. Gaussian SH pulse with duration of 100 fs. Although for the domain size we adopted a coarse resolution of 100 nm, two orders of magnitude larger than what achievable with the algorithm, we obtained an excellent convergence to desired profile and conversion efficiency. Figure 5(b) plots the results for case (ii), a 150 fs pulse. Noticeably, the required grating length increased as compared to the previous case, with a non-monotonic energy exchange between FF and SH in propagation. Figure 5(c) displays the results for (iii), a 200 fs target pulse. The grating is even longer than above; the agreement between target and output pulses is quite satisfactory, despite the small but appreciable discrepancy between their PG-FROG traces. This stems from the high accuracy of the PG-FROG traces used in calculating the RMS error. The results above demonstrate the good performance of the algorithm when simple Gaussian SH pulses are desired at the output, owing to the lack of sharp (temporal or spectral) features.

#82198 - $15.00 USD Received 17 Apr 2007; revised 26 May 2007; accepted 27 May 2007; published 1 Jun 2007

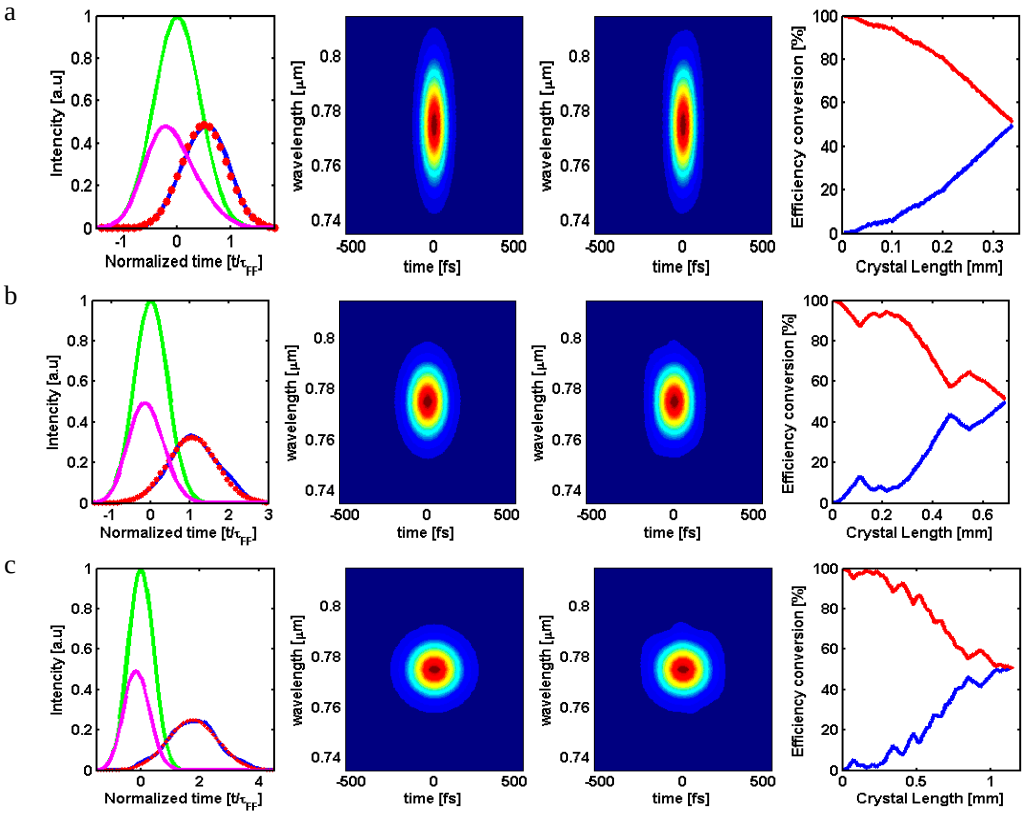

Fig. 5. Left: FF intensity distributions (green (ξ=0), magenta (ξ=ξ_o)), desired target profile (•) and obtained SH profile (blue). Center: PG-FROG spectrograms of target (center left) and final (center right) SH pulses. Right: FF (red) and SH (blue) power versus propagation length. (a) case (i) with a flat phase Gaussian pulse of 100 fs; (b) case (ii) with a 150 fs pulse; (c) case (iii) with 200 fs duration.

In Fig. 6 we display the results concerning more complex targets. In Fig. 6(a) we obtained the double-hump pulse of case (iv) and in Fig. 6(b) the case (v). A few cascaded conversion processes are required to reach the desired SH profiles, with a satisfactory agreement in both PC-FROG traces and temporal behavior between targets and outputs.

#82198 - $15.00 USD Received 17 Apr 2007; revised 26 May 2007; accepted 27 May 2007; published 1 Jun 2007

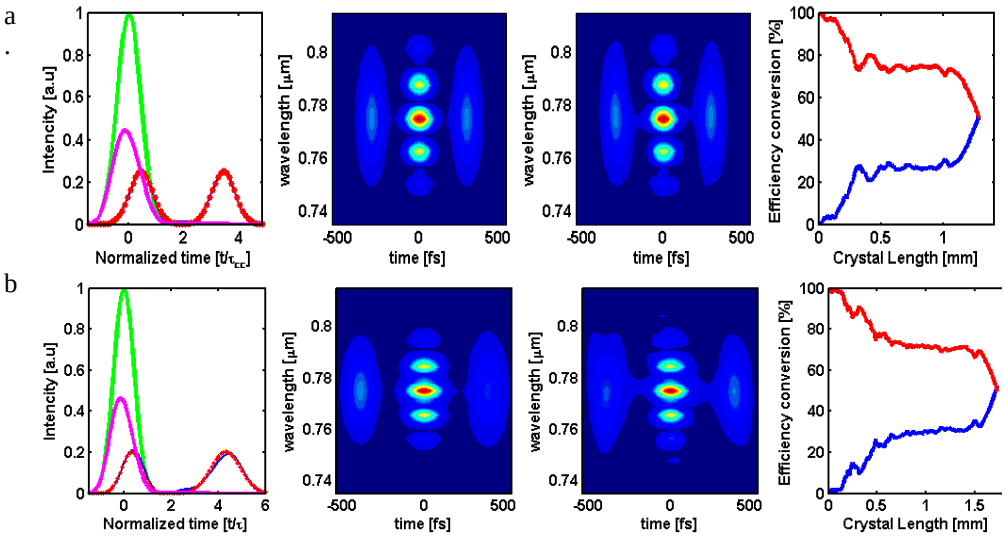

Fig. 6. Left: FF intensity distributions (green (ξ=0), magenta (ξ=ξo)), desired target profile (•) and obtained SH profile (blue). Center: PG-FROG spectrograms of target (center left) and final (center right) SH pulses. Right: FF (red) and SH (blue) power versus propagation length. (a) Case (iv) with two equal width pulses; (b) case (v) with two unequal width pulses of 100 and 200 fs, respectively.

It is also interesting to create SH pulses with a linear phase variation. Figure 7(a-b) summarizes the results for cases (vi) and (vii) above, with positive and negative chirp superimposed on 100 fs pulses at SH, respectively. Despite the slight discrepancy in the PC-FROG traces, the algorithm operated well for such small chirps. Higher chirp rates required much longer run-times and propagation lengths.

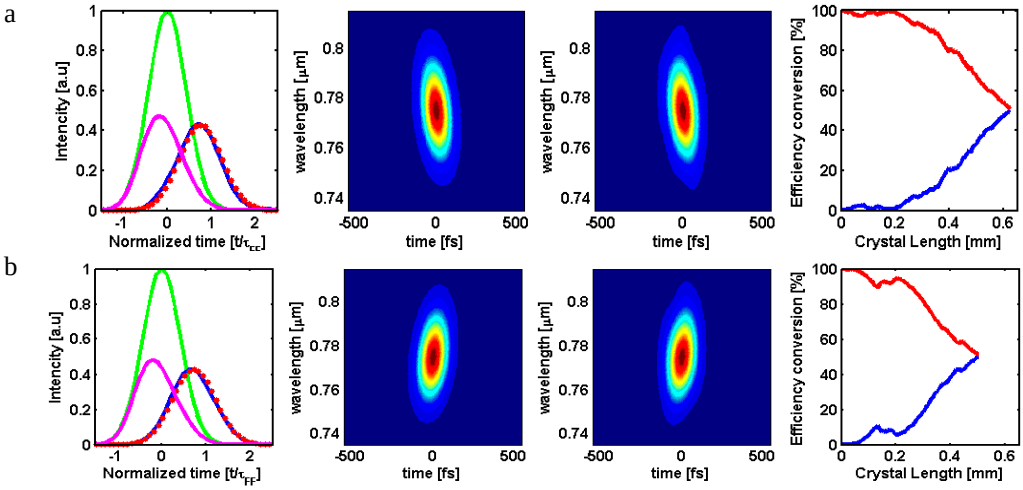

Fig. 7. Left: FF intensity distributions (green (ξ=0), magenta (ξ=ξ$_o$)), desired target profile (•) and obtained SH profile (blue). Center: PG-FROG spectrograms of target (center left) and final (center right) SH pulses. Right: FF (red) and SH (blue) power versus propagation length. (a) Case (vi) with positive chirp ~150 fs^2 on a 100 fs pulse; (b) case (vii) with negative chirp ~ -150 fs^2.

#82198 - $15.00 USD Received 17 Apr 2007; revised 26 May 2007; accepted 27 May 2007; published 1 Jun 2007

Figure 8 plots the distribution of domain sizes throughout the grating length for the various targets synthesized above. Contrary to intuition, the domains appear to be distributed rather non-homogeneously: this unexpected result stems from large pump depletion, as the latter tends to break the "quasi-linear" approximation characteristic of low conversion efficiencies.

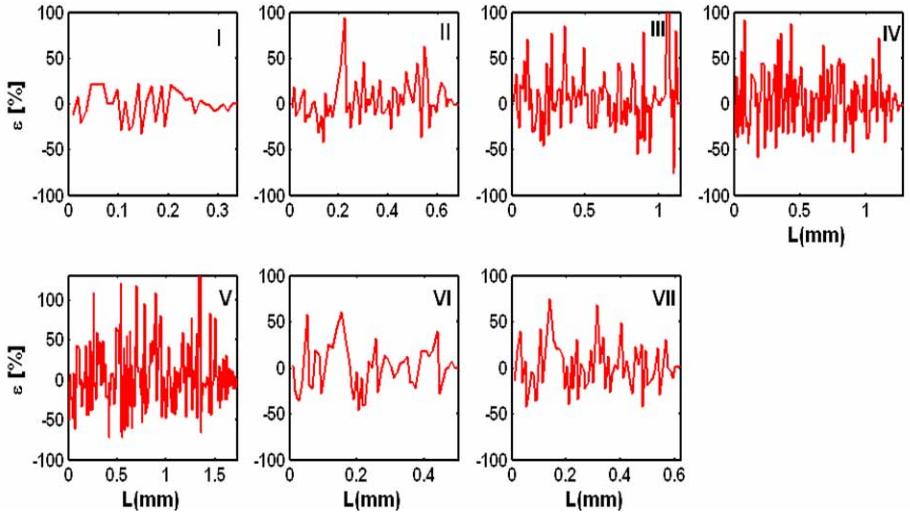

Fig. 8. Domain size distribution along the crystal and corresponding number of domains N for the seven target profiles: (i) 100 fs Gaussian, N=37; (ii) 150 fs Gaussian, N=75; (iii) 200 fs Gaussian, N=120; (iv) 100 fs twin-pulses with a separation of 300 fs, N=135; (v) 100 and 200fs pulses with a separation of 400 fs, N=185; (vi) a positively chirped 100 fs Gaussian pulse (ϕ'' ~150 fs^2), N=54; (vii) a negatively chirped 100 fs Gaussian pulse (ϕ'' ~-150 fs^2), N=66.

Finally, in order to address the issue of practical fabrication tolerances, the graphs in Fig. 9 show the SH profiles of case (iv) as obtained by varying the domain resolution in the SAA algorithm.

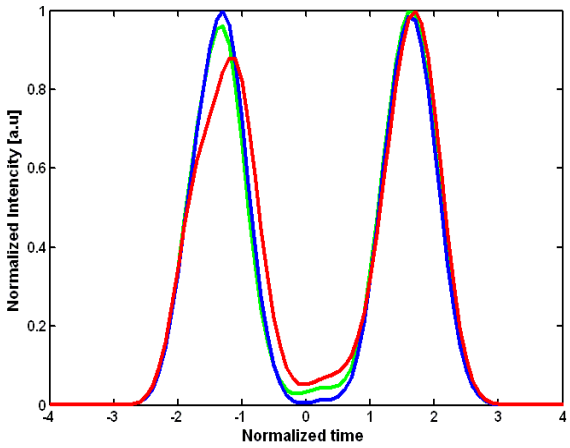

Fig. 9. Calculated SH pulse shape with different resolution in domain size: 100 nm (blue line), 500 nm (green line), 1 μm (red line).

#82198 - $15.00 USD Received 17 Apr 2007; revised 26 May 2007; accepted 27 May 2007; published 1 Jun 2007

5. Conclusions

In conclusion, using the simulated annealing algorithm, we were able to synthesize a variety of femtosecond pulse profiles through second-harmonic generation of a 100 fs Gaussian input at the fundamental frequency. PG-FROG spectrograms were used to calculate RMS errors and lead to rapid convergence of the method with high accuracy. The results, outlined for the relevant case of an aperiodically poled Lithium Niobate crystal, demonstrate that proper engineering of a quasi-phase-matched grating is feasible even under severe pump depletion and in the presence of limited fabrication resolution.

Acknowledgments

This work was supported by Italian MIUR (PRIN 2005098337) and EU project “POISE” no. 512450.

#82198 - $15.00 USD Received 17 Apr 2007; revised 26 May 2007; accepted 27 May 2007; published 1 Jun 2007